



A triband EBG loaded microstrip fractal antenna for THz application

S.K. Vijay^a, J. Ali^{b,1}, P. Yupapin^{c,d,2}, B.H. Ahmad^e, and K. Ray^{f,*}

a. *Department of Electronics & Communication Engineering, Amity University, Jaipur, Rajasthan, India.*

b. *Department of Physics, Institute of Advanced Photonic Science, University Teknologi, Malaysia.*

c. *Computational Optics Research Group, Advanced Institute of Materials Science, Ton Duc Thang University, District 7, Ho Chi Minh City, Vietnam.*

d. *Faculty of Applied Sciences, Ho Chi Minh City, District 7, Ton Duc Thang University, Vietnam.*

e. *Faculty of Electronic and Computer Engineering, University Teknikal Malaysia Melaka, Melaka, Malaysia.*

f. *Department of Physics, Amity University Rajasthan, Jaipur, India.*

Received 28 October 2020; received in revised form 29 May 2021; accepted 20 September 2021

KEYWORDS

Electronic band gap;
 Terahertz antenna;
 Microstrip fractal antenna;
 Monolithic microwave integrated circuit.

Abstract. Future wireless communication needs antennas with multifunctional operation. This paper focuses on *Terahertz Antenna* that could be easily integrated with micro and nano devices. In this paper, an octagonal shaped *Microstrip Fractal Antenna* loaded with the EBG structure is designed for tri-band terahertz application. Triple band characteristic achieved by fractal radiating patch is loaded with *Electronic Band Gap (EBG)*. The antenna features total size of $700 \times 900 \mu\text{m}^2$ and resonates on three bands at 0.948 THz, 0.984 THz, and 1.040 THz. The result and performance indicates that the recommended antenna will be suitable for compact wireless devices and *Monolithic Microwave Integrated Circuit (MMIC)*. All simulation works have been completed using electromagnetic software Ansoft High-Frequency Structure Simulator (HFSS) and CST studio suite. The electromagnetic features like S11 parameters, VSWR, gain, efficiency, and radiation characteristics of the suggested antenna are also examined. The simulation results show that this antenna has 9 dB realized gain at a resonating frequency of 0.948 THz.

© 2023 Sharif University of Technology. All rights reserved.

1. Introduction

Technological advancement and immense demand for wireless devices have compelled manufacturers and

researchers to develop cheap, small-sized, low-visibility, and broadband planar antennas. Terahertz band had inspired many researchers due to un-licensed use with its small size, low visibility, compactness, and high data rates [1]. The need for high-speed data rate is raising rapidly and will influence the wired communication capacity limit much quickly. The coming generation would require data rate better than 100 Gbps, maintaining the necessity of investing additional frequency band for wireless communication [2]. A special frequency band ranging from 100 to 10 k gigahertz termed as the terahertz band is considered to be essential for answering the increasing data rate demand [2]. Several kinds of research have investigated the implementation

1. *Present address: Asia Metropolitan University, 6, Jalan Lembah, Bandar Baru Seri Alam, 81750 Masai, Johor, Malaysia.*

2. *Present address: Department of Electrical Technology, Faculty of Industrial Technology, Institute of Vocational Education Northeastern 2, Sakonnakhon, 47000, Thailand.*

*. *Corresponding author.*
E-mail address: kanadray00@gmail.com (K. Ray)

of microstrip antennas at optical frequency bands over the last few years [3–17].

Optical antennas have been found in various applications like single-band operation [1], triple-band [2], wide-band [3,4], and multi-band applications [5] as well as WBAN [7,8], Bio-sensing [11], dual polarization [12], etc.

Due to low carrier mobility, the optical antenna suffers many challenges like deficient gain, harsh attenuation, and extremely weak efficiency that affect the commercial implementation of THz wireless communication systems [6]. Likewise, the low plasma frequency, high electron mobility, and the field-effect of graphene make it a relevant element for producing high-frequency nano-electronic devices [9–12]. Band gap structures categorized in optical and electrical studies have been used for designing so that the path loss could be reduced and antenna parameters enhanced [13]–[16].

Miniaturization is the inherent requirement for terahertz frequency range devices and fractal antennas suit the circumstances. The uniqueness of fractal geometry self-relation and space-filling ability led to size miniaturization and wider bandwidth [17,18]. Researchers introduced many fractal geometries for

practical antenna design like hexagonal fractal patch [19], honeycomb shaped [20], sunflower shaped [21,22], and elliptical fractal antenna [23]. The self-similar structure of octagon geometry is more suitable for fractal geometry. As compared with circular patch antenna, the octagon can fill more metallic area in a plane [24]. In fractal geometries, octagonal shapes would be preferred over circular shape because it occupies the entire region without overlapping. Good gain and bandwidth performance are other reasons to consider octagon [25]. Table 1 lists the comparison between the proposed design and different existing designs in the literature. Here, as shown in Table 1, some important parameters like substrate material, antenna size, working frequency band, gain as well as application of the reported literatures are compared with the recommended antenna.

Future wireless device application needs compact design and multi-band operation [5]. Multiband characteristics facilitate shrinking the space and weight while incorporating with MMIC. To address the above issue in this paper, an octagonal shaped fractal antenna is proposed with triple band characteristics for 948 GHz, 984 GHz, and 1040 GHz. The overall antenna dimension is $700 \times 900 \mu\text{m}^2$. To enhance the perfor-

Table 1. Comparison of the proposed antenna with existing antennas.

Ref. no.	Substrate material (ϵ_r)	Size (μm)	Resonant frequencies (THz)	Gain (dB)	State of Art
[1]	Pyrex, $\epsilon_r = 5.2$	430*430	2.3	12.67	Anomaly detection
[2]	SiO ₂ , $\epsilon_r = 4.0$	40*40	2.25	4.75 & 4.3	Moving target tracking
[3]	Polyamide, $\epsilon_r = 4.3$	600*800	22.5	10.82	WBAN application
[4]	Polyamide, $\epsilon_r = 4.3$	600*800	2.9	9.44	WPAN application
[5]	SiO ₂ , $\epsilon_r = 3.9$	50*50	1.9, 4.83 & 5.55	4.75 & 4.3	Graphene patch
[6]	Glass, $\epsilon_r = 6.0$	50*30	1.425	–	Transparent conductor oxide materials
[7]	RT Duriod(6010) $\epsilon_r = 10.2$	200*200	0.852	2.5	WBAN application
[8]	RT Duriod 6010 /Si $\epsilon_r = 10.2$	100*100	2.270	4.8	WBAN application
[9]	SiO ₂ , $\epsilon_r = 4.0$	14*14	12.2-13.8	5.30	Graphene based patch
[10]	Si, $\epsilon_r = 11.0$	24*24	5.5	3.9	Graphene patch
Proposed design	RT Duriod (6010) $\epsilon_r = 10.2$	700*900	0.948, 0.984 & 1.04 (triple band)	9	Wireless application

mance, an EBG structure is embedded near the radiating patch. An octagonal-shaped microstrip antenna structure is examined to design terahertz antenna with a triple band. Since the primary antenna radiates at high frequency, various iterations are applied in order to form a fractal antenna. Finally, an EBG structure is embedded near the radiating geometry and feed line to create triple band characteristics. The entire work is arranged as follows. The primary antenna design, analysis, and synthesis are described in Section 2. Section 3 describes and validates the result of fractal geometry. EBG structure has been implemented to design triple band antennas described in Section 4, followed by different conducting material analysis. Finally, the conclusion of the article is described in Section 5. All simulation works are performed using electromagnetic software like Ansys HFSSv15 and CST software.

2. Octagonal radiating patch (primary antenna)

The octagonal patch antenna is closely associated with the circular patch antenna. Therefore, a circular patch design equation must be introduced first to calculate the design equation. The theoretical resonance frequency of a circular patch antenna is specified by authors in [26]:

$$F = \frac{8.791 \times 10^9}{fr\sqrt{\varepsilon_r}}, \quad (1)$$

where F is constant, fr is resonating frequency in Hz, and ε_r is dielectric constant of the substrate. The radius ' r ' of the circular patch can be calculated as follows:

$$r = \frac{F}{1 + \frac{2h}{\pi\varepsilon_r F} [\ln(\frac{\pi F}{2h}) + 1.7726]}^{1/2}, \quad (2)$$

where h is the height of substrate. Therefore, the effective radius ' r_e ' can be defined as follows:

$$r_e = r \left\{ 1 - \frac{2h}{\pi r \varepsilon_r} \left(\ln \frac{\pi r}{2h} + 1.7726 \right) \right\}^{0.5}. \quad (3)$$

These equations (Eqs. (1) to (3)) can be implemented for creating a circular microstrip patch antenna. As can be seen from Figure 1, the radius of the octagon is equal to that of the circle. Thus, the side lengths of the octagonal patch can be calculated based on the effective area of the circular patch in Eq. (4):

$$\pi r_e^2 = 2(1 + \sqrt{2})s^2. \quad (4)$$

The radius of patch geometry can be calculated using the formula of side length in Eq. (4). Initially, the radius of octagonal radiating patch was chosen as 250 μm . An octagonal-shaped patch is designed on

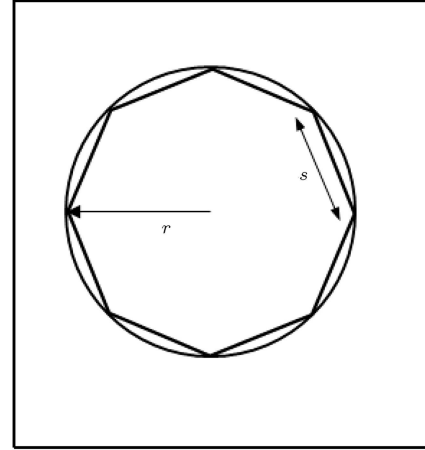


Figure 1. Realization of octagonal and circular patches.

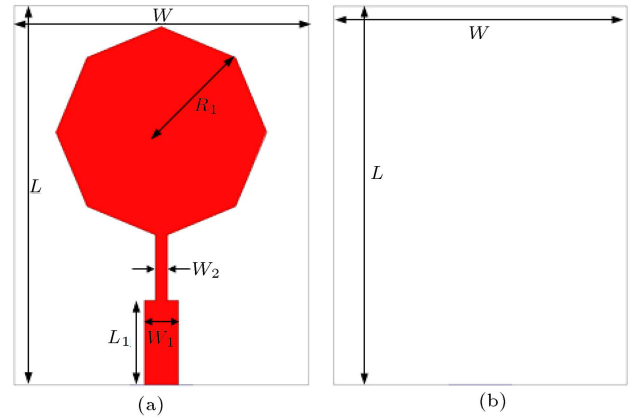


Figure 2. Primary octagonal antenna: (a) Front side and (b) back side.

Table 2. Optimized dimensions of the primary antenna.

Parameter	R_1	L	W	L_1	W_1	W_2
Unit (μm)	250	900	700	150	80	30

the top of the Rogers RT/Duroid 6010 substrate with a dielectric constant (ε_r) of 10 and loss tangent of 0.0023. The optimized antenna is fed with an 80 μm wide microstrip feed line to achieve 50 Ω characteristics impedance matching between patch and feed line. For better impedance matching, quarter transmission of 30 μm width was designed. This octagon-shaped optical antenna is depicted in Figure 2. The radiating element combined with the conductive ground plane and also the proposed antenna can support the large operating band with multiple resonances. The entire dimensions described in Figure 2 are listed in Table 2.

Simulated results in terms of reflection coefficient (S_{11} in dB) are shown in Figure 3. It can be well examined from the plot in Figure 3 that the antenna has impedance matching at a resonance frequency of 0.992 THz with S_{11} value of -17dB using microstrip

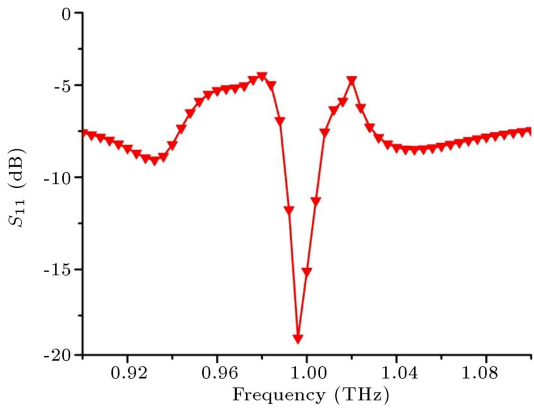


Figure 3. Simulated S_{11} (dB) of the suggested antenna.

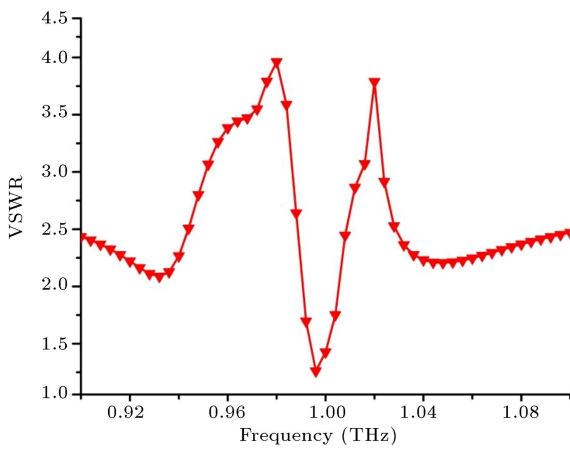


Figure 4. Simulated VSWR of the primary antenna.

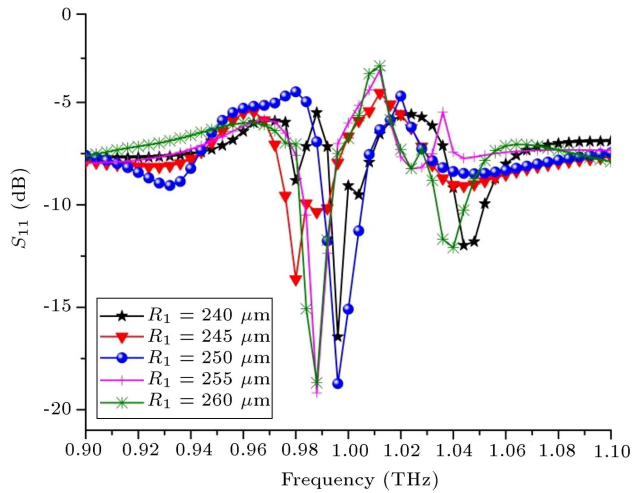


Figure 5. Primary antenna radius variation.

line feed and quarter wave transformer. The S_{11} results confirm that the primary antenna resonates at 0.992 THz frequency. In Figure 4, VSWR versus frequency plot shows less than 2 VSWR value. The obtained VSWR at a simulated frequency of 0.992 THz is 1.3.

After obtaining the scattering parameter, the radius ' R_1 ' of octagon varied and the result is shown in Figure 5. According to this figure, it can be seen

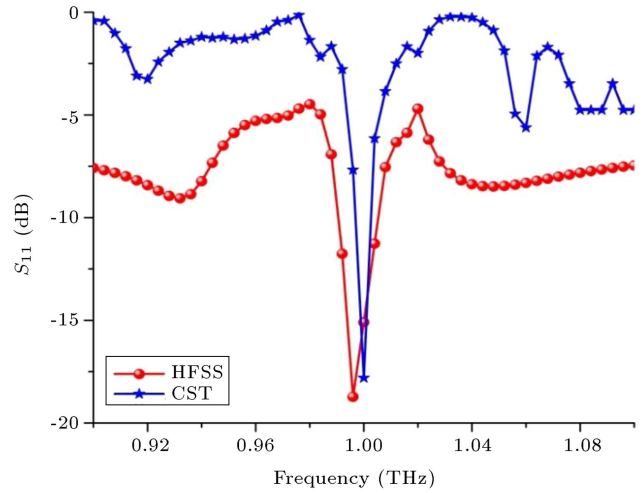


Figure 6. Simulated S_{11} (dB) comparison.

Table 3. Optimized dimensions of the primary antenna.

Parameter	R_2	R_3	R_4
Unit (μm)	222	188	155

that frequency shifted towards lower band while increasing the radius of octagon geometry. At a radius of 250 μm , the antenna provides better impedance matching.

The simulated S_{11} parameters are also verified in Figure 6, where the HFSS value is compared with CST software. Values in Figure 6 indicate satisfactory antenna performance.

3. Fractal shaped octagonal antenna

The primary antenna produces only single band characteristics. To achieve the multiband performance, various iterations are loaded to create fractal geometry. The fractal geometry is designed by loading multiple octagonal slots in the radiating geometry at its center. For achieving the first iteration, an octagon with a radius of 222 μm scaled down is considered. Further, after adding an octagonal geometry, the next iteration ensues. The fractal geometry is analyzed until the 3rd iteration to find the truthful performance. Further iterations are not presented due to antenna performance degradation and geometry complexation at the corresponding higher iterations.

Figure 7 represents the fractal antenna geometries. The inner radii of all the fractal iterations are listed in Table 3.

The intermediate antenna configuration steps are reviewed and represented in Figure 8 and also listed in Table 4. It is observed that at the initial three iterations, the resonant frequency shifts towards a higher frequency band. After that, the bandwidth

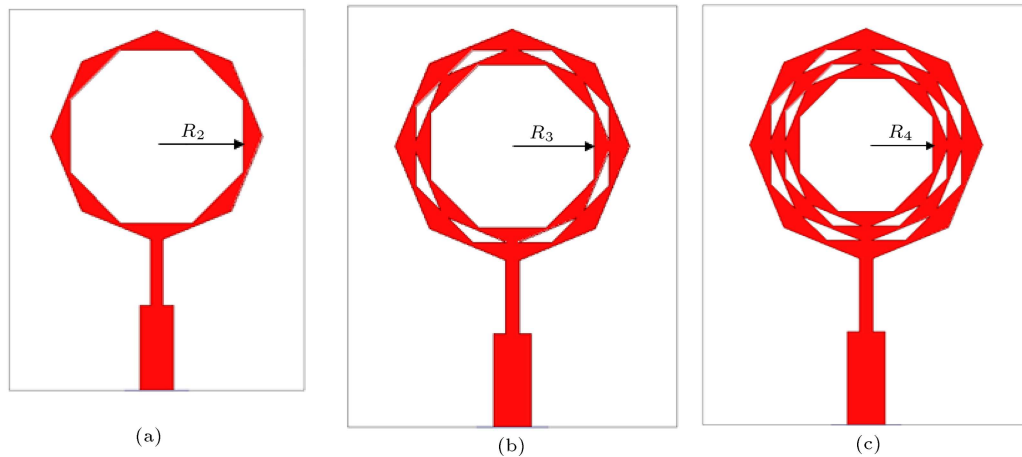


Figure 7. Development of fractal antenna: (a) Antenna-I (1st iteration), (b) Antenna-II (2nd iteration), and (c) Antenna-III (3rd iteration).

Table 4. Comparative results of the proposed antenna.

Geometry	Frequency band (GHz)	Resonating frequency (GHz)	Gain (dBi)
1st iteration	981–991 & 1031–1040	984 & 1036	3.65 & 5.75
2nd iteration	982–990 & 1031–1040	984 & 1036	5.66 & 4.33
3rd iteration	980–992 & 1026–1041	984 & 1032	3.2 & 4.2

decreases due to variation in gap capacitance. Finally, the increase of the iterations shifts the operating frequencies to the higher frequency band.

The scattering parameters obtained from HFSS software are also compared with those from CST software in Figure 9. Figure 9 displays good agreement between the obtained results.

4. EBG design loaded with fractal antenna

The fractal geometry provides dual band characteristics. Triple band resonance is generated when octagonal fractal shape is applied with SMEBG structure. A pair of Square Mushroom EBG (SMEBG) cells embedded near the quarter wave transmission line, as displayed in Figure 10, has been adopted for multiband characteristics improvement. To create the third band, we have recommended an SMEBG cell which is grounded using metallic via. The entire size of the SMEBG cell is $150 \times 150 \mu\text{m}^2$. The entire dimensions of the arrangement displayed in Figure 10 are listed in Table 5.

Table 5. Optimized dimensions of the proposed antenna.

Parameter	L_2	W_3	Via
Unit (mm)	150	150	20

The required triple band at 0.948 THz, 0.984 THz, and 1.040 THz is realized by applying the SMEBG structure in the fractal-shaped octagonal antenna. Figure 11 indicates that antenna provides extra resonance at 0.948 THz with a reflection coefficient of -15 dB. The proposed antenna provides three bands at the center frequency of 0.948 THz, 0.984 THz, and 1.040 THz with S11 of -15 dB, -19.34 dB, and -21.42 dB. This design shows very good bandpass characteristics at 0.948/0.984/1.04 THz, which can be seen in Figure 11. This could also be seen in Figure 12, where VSWR is below 2. The values of VSWR at 0.948 THz, 0.984 THz, and 1.04 THz are 1.55, 1.40, and 1.45, respectively. The VSWR value indicates excellent bandpass properties.

After analyzing the suggested antenna characteristics, the width and length of EBG structure varied to find optimum dimensions. In Figure 13, W_2 is kept constant and length of EBG structure is varied according to the value of ' L_2 '. Further width ' W_2 ' of the EBG structure also varies and the variation is plotted in Figure 14.

Figure 15 shows the surface current distribution on the proposed antenna geometry at desired resonating frequencies of 0.948 THz, 0.984 THz, and 1.040 THz. The surface current is uniform and is concentrated at fractal edges. The uniform vector current verified pass band features on resonant frequency.

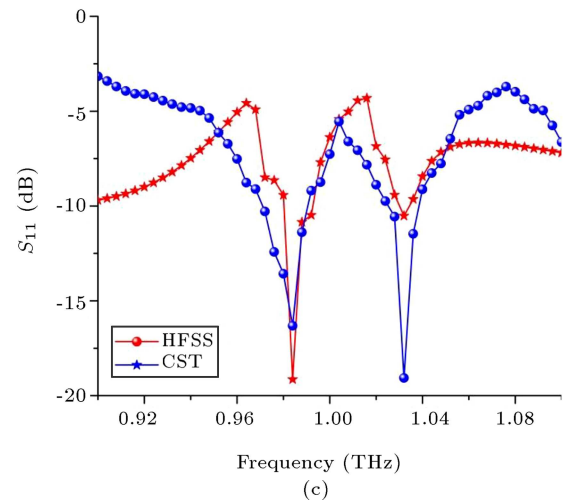
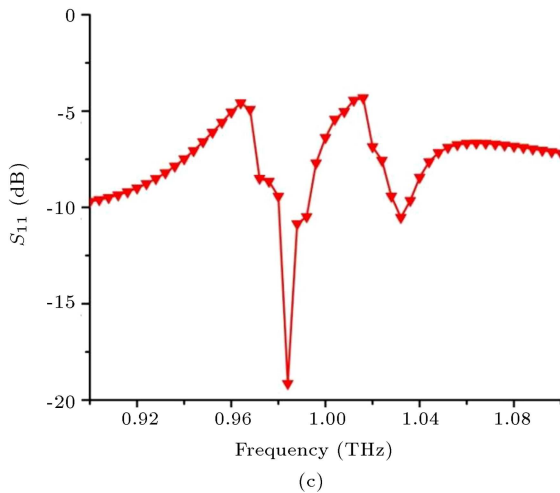
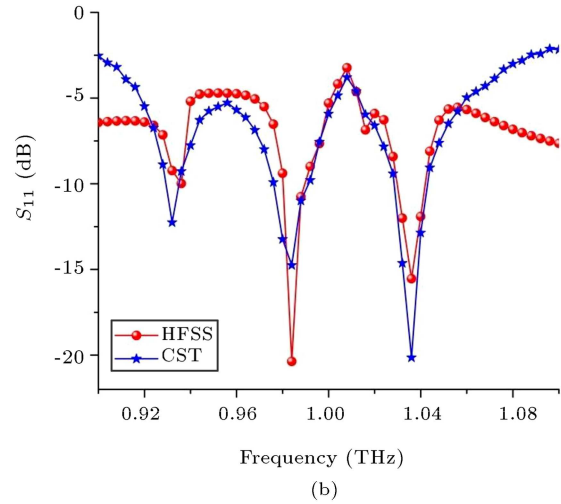
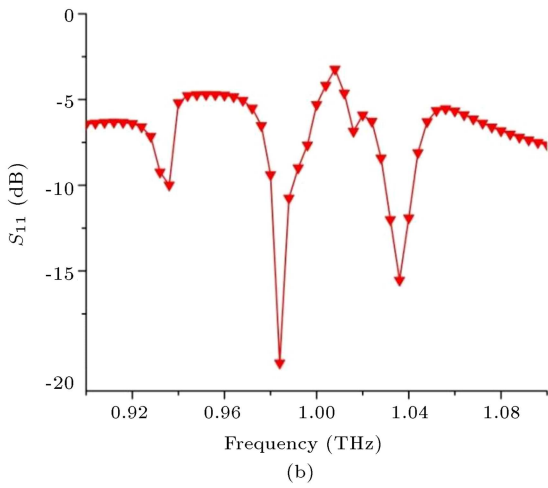
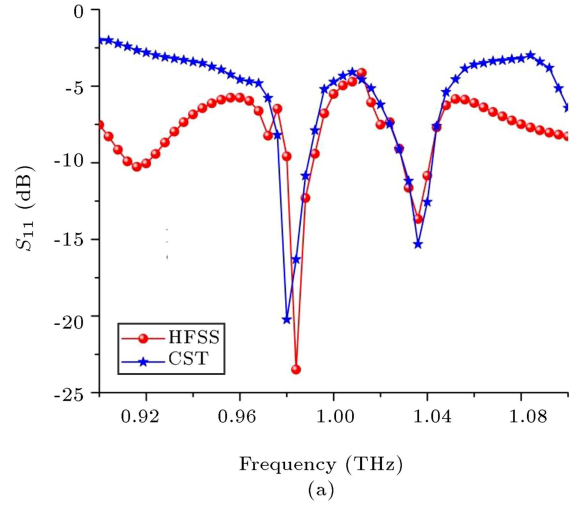
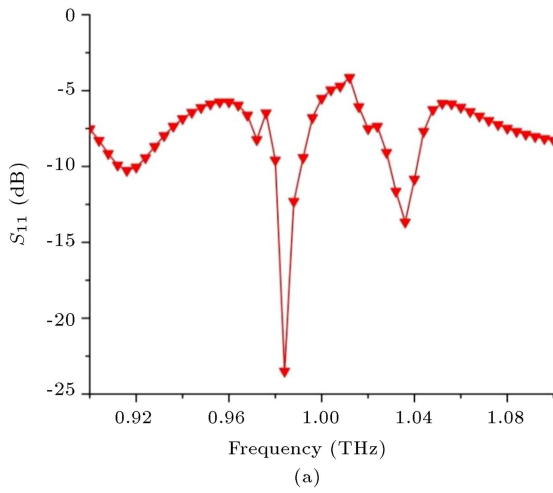


Figure 8. Simulated S_{11} (dB) of suggested antennas: (a) Antenna-I, (b) Antenna-II, and (c) Antenna-III.

Figure 9. Compared S_{11} (dB) of fractal antenna: (a) Antenna-I, (b) Antenna-II, and (c) Antenna-III.

The radiation and gain characteristics may also prove these features. The radiation pattern of the presented antenna satisfies passband characteristics with appropriate matching results, as shown in Figure 16.

Antenna gain characteristics are shown in Figure 17. It can be observed that gain is approximately around 1.20 dB for 984 GHz frequency and 2.37 dB at 1040 GHz frequency, whereas 9 dB for 948 GHz. However,

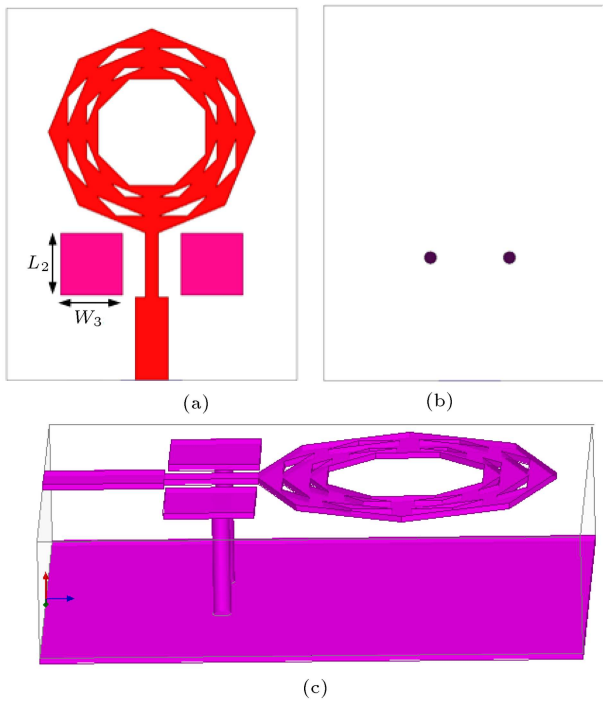


Figure 10. Triple band fractal antenna: (a) Front side, (b) back side, and (c) perspective view.

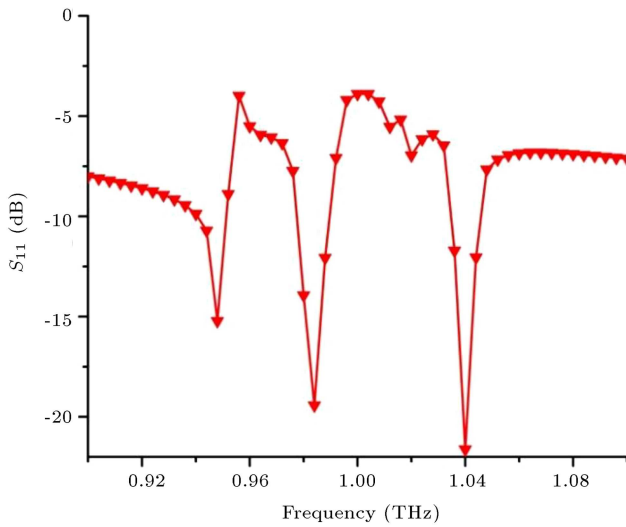


Figure 11. Simulated S_{11} (dB) of the suggested antenna.

antenna gain can also be compared with other works of literature in Table 6.

According to the results provided in the table, the gain of the antenna is considerably greater than those of other antennas specified in the table. This above analysis can show good reasons when the antenna is installed in the areas of demand.

The gain, VSWR, and S_{11} parameter of the final antenna are also verified with CST software. The compared graph is displayed in Figures 18, 19, and 20. The discrepancy in the result of both simulators results from different mesh sizes and analytical techniques.

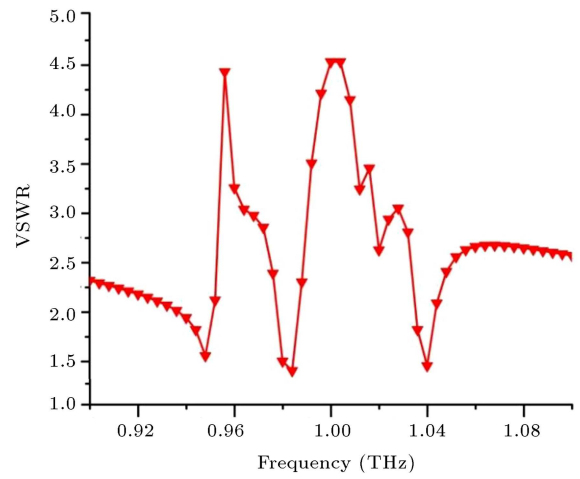


Figure 12. Simulated VSWR of the suggested antenna.

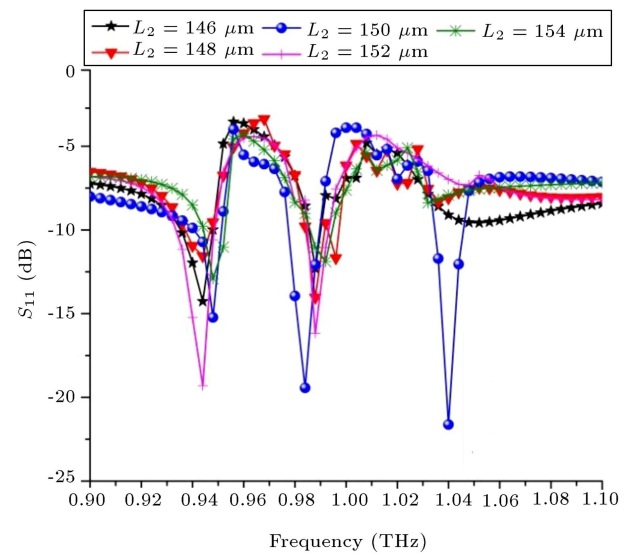


Figure 13. EBG length variation.

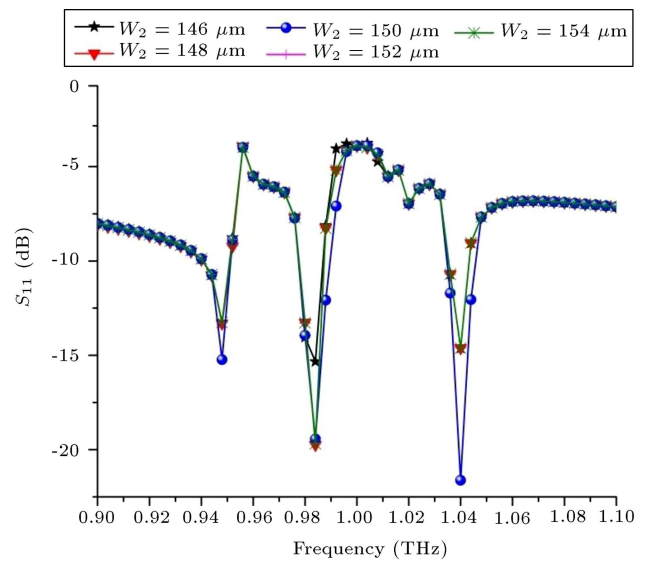


Figure 14. EBG width variation.

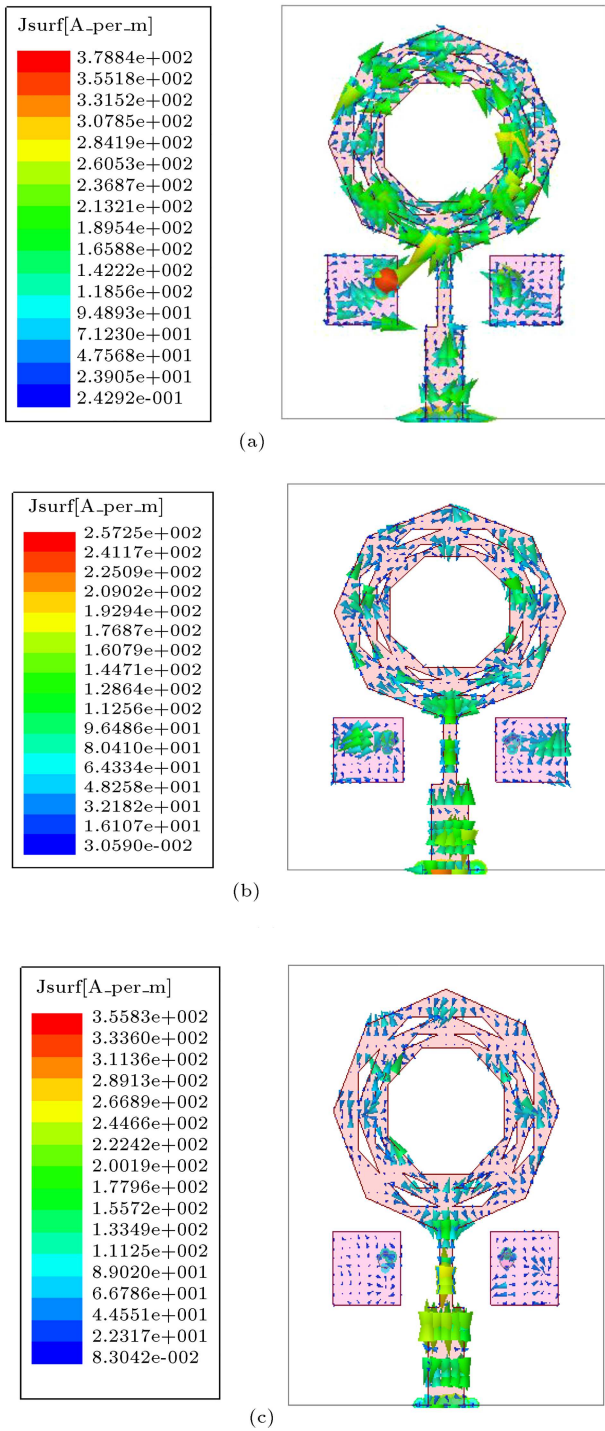


Figure 15. Current distribution of the proposed antenna: (a) 948 GHz, (b) 984 GHz, and (c) 1040 GHz.

Some other conductors such as silver with conductivity of 0.61×10^8 Siemens/m and mass density of 10500 and gold with conductivity of 0.41×10^8 Siemens/m and mass density of 19300 are used to produce optical antennas after developing the triple band antenna in THz band. The antenna frequency is highly dependent on the material conductivity.

Figure 21 illustrates that resonating frequency

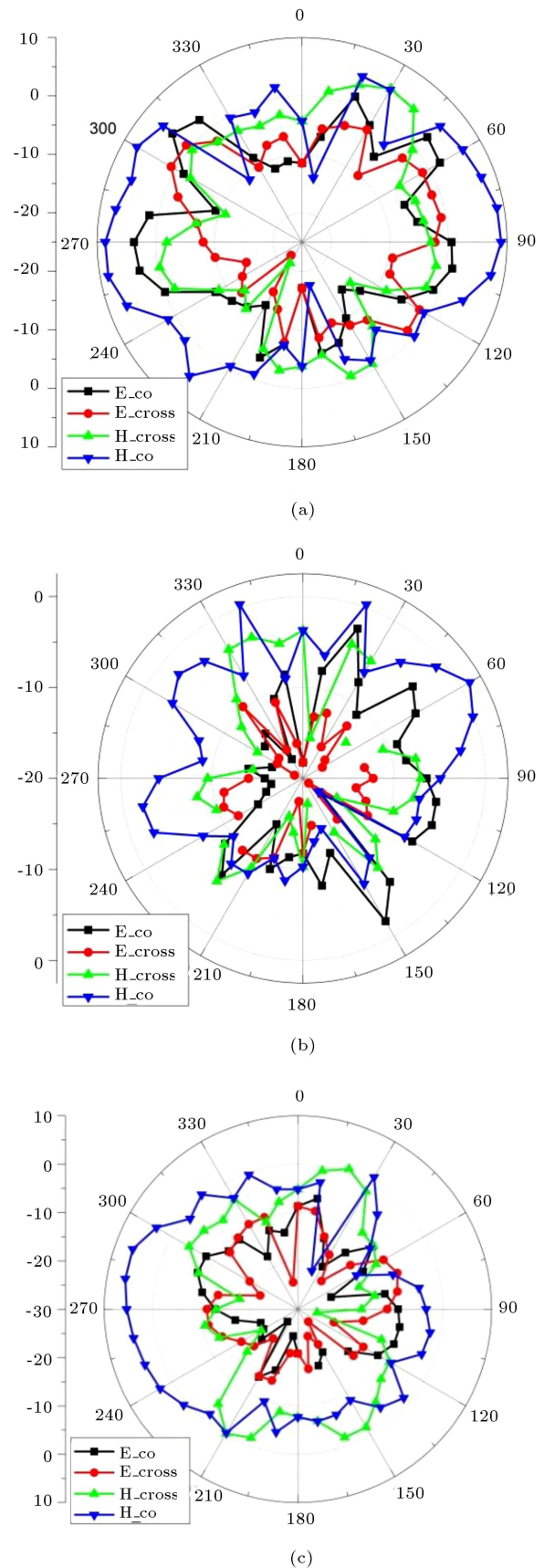


Figure 16. Radiation pattern of the proposed antenna: (a) 948 GHz, (b) 984 GHz, and (c) 1040 GHz.

Table 6. Comparison of antenna parameter with other existing antennas.

Antenna	Proposed antenna	Antenna-III	[7]	[8]	[9]	[10]
Gain (dB)	9	4.2	2.5	4.8	5.3	3.9

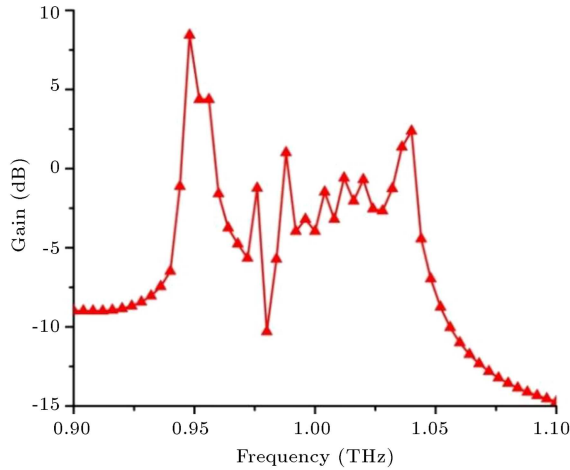


Figure 17. Realized peak gain vs. frequency graph.

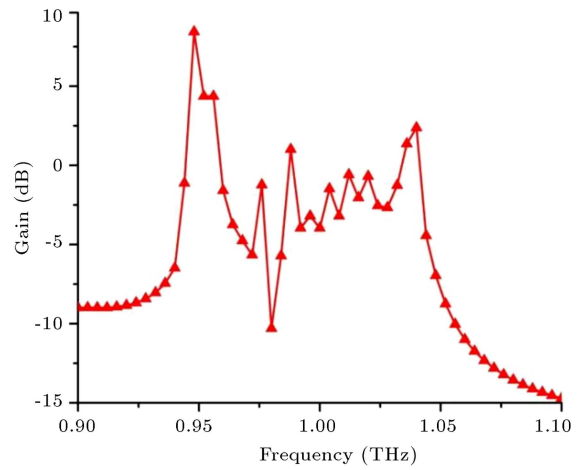


Figure 20. Compared gain vs. frequency of the final antenna.

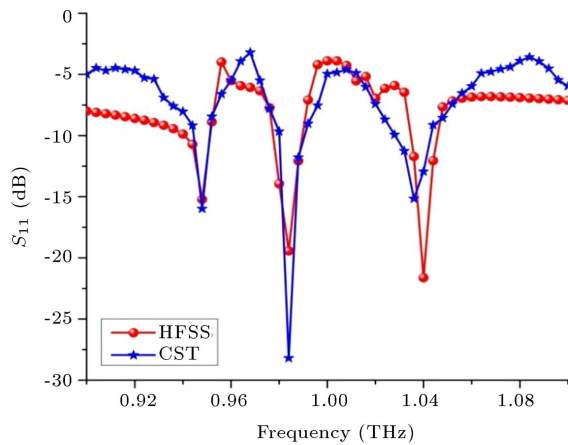


Figure 18. Compared S_{11} (dB) vs. frequency of the final antenna.

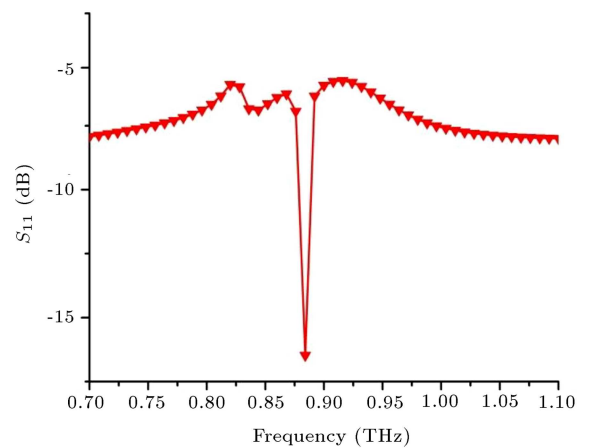


Figure 21. Simulated S_{11} (dB) of the suggested antenna loaded with silver.

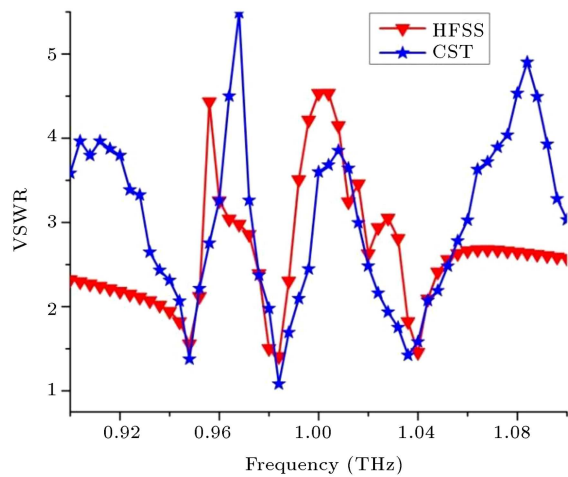


Figure 19. Compared VSWR vs. frequency of the final antenna.

shifts towards lower band after using the silver instead of copper. Figure 22 plots the effect of gold material on reflection coefficient. Analysis of various materials may, therefore, be a suitable choice for the broad spectrum of frequency tunings. The simulation indicates that the proposed antenna behaves like metamaterial superstrate.

5. Conclusion

The suggested antenna produced triple band resonance characteristics. Initially, an octagonal microstrip was considered for wireless application. After that, the octagonal slots were introduced to create a fractal-shaped geometry. This fractal geometry accomplished dual band characteristics. Next, electronic band gap

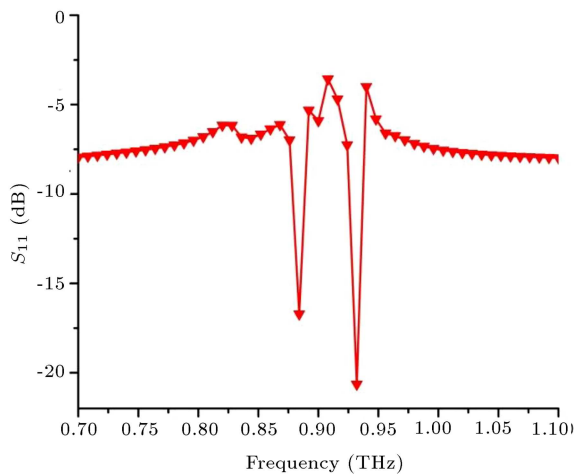


Figure 22. Simulated S_{11} (dB) of the suggested antenna loaded with gold.

structures were embedded near patch to provide a triple band resonance feature. Then, the suggested antenna application was compared with those in the literature. The recommended antenna had a simple structure and a compact size of $700 \times 900 \mu\text{m}^2$. All antenna results indicate that the proposed antenna can be used to operate at three bands for different applications as nano antennas, indoor communications, miniaturized equipment, and WPANs. Finally, the antenna patch is made of some gold and silver, which can fin-tune the frequency features of the antenna.

References

1. Efazat, S.S., Basiri, R., and Makki, S.V.A.D. "The gain enhancement of a graphene loaded reconfigurable antenna with non-uniform metasurface in terahertz band", *Optik*, **183**, pp. 1179–1190 (2019).
2. Bansal, G., Marwaha, A., Singh, A., et al. "A triband slotted bow-tie wideband THz antenna design using graphene for wireless applications", *Optik*, **185**, pp. 1163–1171 (2019).
3. Singhal, S. and Budania, J. "Hexagonal fractal antenna for super wideband terahertz applications", *Optik - International Journal for Light and Electron Optics*, **206**, 163615 (2019).
4. Singhal, S. "Elliptical ring terahertz fractal antenna", *Optik - International Journal for Light and Electron Optics*, **194**, 163129 (2019).
5. Shalini, M. and Madhan, M.G. "Performance predictions of slotted graphene patch antenna for multi-band operation in terahertz regime", *Optik - International Journal for Light and Electron Optics*, **204**, 164223 (2020).
6. Rashed, A.N.Z. and Sharshar, H.A. "Optical microstrip patch antennas design and analysis", *Optik*, **124**, pp. 4331–4335 (2013).
7. Rubani, Q., Gupta, S.H., Pani, S., et al. "Design and analysis of a terahertz antenna for wireless body area networks", *Optik*, **179**, pp. 684–690 (2019).
8. Rubani, Q., Gupta, S.H., and Kumar, A. "Design and analysis of circular patch antenna for WBAN at terahertz frequency", *Optik*, **185**, pp. 529–536 (2019).
9. Bala, R. and Marwaha, A. "Characterization of graphene for performance enhancement of patch antenna in THz region", *Opt. Int. J. Light Electron. Opt.*, **127**(4), pp. 2089–2093 (2016).
10. Khan, M.A., Shaem, K.T.A., and Alim, M.A. "Analysis of graphene based miniaturized terahertz patch antennas for single band and dual band operation", *Optik - International Journal for Light and Electron Optics*, **194**, 163012 (2019).
11. Zarrabi, F.B., Moghadasi, M.N., Heydari S., et al. "Cross-slot nano-antenna with graphene coat for bio-sensing application", *Optics Communications*, **371**, pp. 34–39 (2016).
12. Shalini, M. and Madhan, M.G. "Design and analysis of a dual-polarized graphene based microstrip patch antenna for terahertz applications", *Optik - International Journal for Light and Electron Optics*, **194**, 163050 (2019).
13. Naderi, M., Zarrabi, F.B., Jafari, F.S., et al. "Fractal EBG Structure for shielding and reducing the mutual coupling in microstrip patch antenna array", *International Journal of Electronics and Communications*, **93**, pp. 261–267 (2018).
14. Ren, J., Deng, Y., Shi, Y., et al. "Optically controlled reconfigurable terahertz waveguide filters based on photo-induced electromagnetic band gap structures using mesa arrays", *OSA Continuum*, **1**, pp. 1429–1436 (2018).
15. Hocinia, A., Temmara, M.N., Khedrouchea, D., et al. "Novel approach for the design and analysis of a terahertz microstrip patch antenna based on photonic crystals", *Photonics and Nanostructures - Fundamentals and Applications*, **36**, 100723 (2019).
16. Rahmati E. and Boroujeni, M.A. "Design of terahertz photoconductive antenna arrays based on defective photonic crystal substrates", *Optics and Laser Technology*, **114**, pp. 89–94 (2019).
17. Singhal, S., Jaiverdhan, and Singh, A.K. "Elliptical monopole based super wideband fractal antenna", *Microw. Opt. Technol. Lett.*, **62**, pp. 1324–1328 (2020).
18. Krzysztofik, W.J. "Fractals in antennas and metamaterials applications", *Fractal Analysis - Applications in Physics, Engineering and Technology*, pp. 45–81 (2017).
19. Garhwal, A., Ahmad, M.R., Ahmad, B.H., et al. "Mechanically reconfigurable hexagonal fractal patch antenna for ambient computing", *International Journal of Innovative Technology and Exploring Engineering (IJITEE)*, **8**(6), pp. 1478–1484 (2019).
20. Keshwala, U., Rawat, S., and Ray, K. "Honeycomb shaped fractal antenna with defected ground structure

for UWB applications”, *2019 6th International Conference on Signal Processing and Integrated Networks (SPIN)*, Noida, India, pp. 341–345 (2019).

21. Singhm P., Ray, K., and Rawat, S. “Analysis of sun flower shaped monopole antenna”, *Wireless Personal Communications*, **104**(3), pp. 881–894 (2019).
22. Garhwal, A., Ahmad, M.R., Ahmad, B.H., et al. “Circular and elliptical shaped fractal patch antennas for multiple applications”, *International Journal of Engineering and advanced Technology (IJEAT)*, **8**(5), pp. 114–120 (2019).
23. Singh, P., Ray, K., and Rawat, S. “Nature inspired sunflower shaped microstrip antenna for wideband performance”, *International Journal of Computer Information Systems and Industrial Management Application*, **8**, pp. 364–371 (2016).
24. Vivek, R., Yamuna, G., Suganthi, S., et al. “Performance analysis of novel compact octagonal shaped fractal antenna for broadband wireless applications”, *Wireless Pers Commun*, **103**, pp. 1325–1340 (2018).
25. Tripathi, S., Mohan, A., and Yadav, S. “A multinoched octagonal shaped fractal UWB antenna”, *Microw. Opt. Technol. Lett.*, **56**, pp. 2469–2473 (2014).
26. Kushwaha, N. and Kumar, R. “Design of slotted ground hexagonal microstrip patch antenna and gain improvement WITH FSS screen”, *Progress in Electromagnetics Research B*, **51**, pp. 177–199 (2013).

Biographies

Shankar Kumar Vijay is a PhD Scholar in Electronics and Communication Department of Amity University Rajasthan (AUR), Jaipur, India. He has done his B.Tech in ECE from University of Rajasthan, Jaipur and M.Tech in VLSI from Rajasthan Technical University, Kota, Rajasthan. His Research interest are antenna and wave propagation, microwaves devices, UWB antennas and optical antennas.

Jalil Ali received the PhD degree in Plasma Physics from Universiti Teknologi Malaysia (UTM), Skudai, Malaysia in 1990. He was a Professor of Photonics at the Institute of Advanced Photonics Science, Nanotechnology Research Alliance and the Physics Department, UTM and a Visiting Professor at King Mongkut’s Institute Technology Ladkrabang, Bangkok, Thailand. From 1987 to 2010, he held numerous faculty and research positions, including

the Dean/Director, Bureau of Innovation, and Consultancy. He was instrumental in establishing and forging university-industry collaboration in Malaysia. Presently, he is with Asian Metropolitan University, Malaysia.

Preecha Yupapin received the PhD degree in Electrical Engineering from City, University of London, UK in 1993. He is currently a Full Professor in the Computational Optics Research Group, Advanced Institute of Materials Science and a member of the Faculty of Applied Sciences, Ton DucThang University, Ho Chi Minh City, Vietnam. His current researches of interest are nano-devices and circuits, microring resonator, soliton communication, optical motor, quantum communication, and meditation science.

Badrul Hisham Ahmad, currently, has been a Professor of Microwave Engineering at Universiti Teknikal Malaysia, Melaka, since 2018. He received his PhD in Microwave Engineering from University of Leeds, UK. He received his MSc in Electrical, Electronics & System Engineering from UKM, Malaysia. He earned his BEng in Electronics, Communication Engineering from University of Leeds, UK. His research area(s) include microwave filters, dielectric resonators, antennas-switches- DG. He is also an active researcher with a good track record including a number of research projects in RF and microwave engineering. He has published more than 200 journal and conference proceedings. He is a senior member of IEEE and a member of International Steering Committee of Asia Pacific Microwave Conferences.

Kanad Ray has been a Professor of Physics and Electronics & Communication and, presently, is working as the Head of the Department of Physics at the Amity School of Applied Sciences, Amity University Rajasthan (AUR), Jaipur, India. He has done his MSc and PhD in Physics from Calcutta University and Jadavpur University, West Bengal, India, respectively. Prof. Ray’s current research areas of interest include cognition, communication, electromagnetic field theory, antenna and wave propagation, microwave, computational biology, and applied physics. He has been serving as an editor of various Springer Book Series. He was an Associated Editor of Journal of Integrative Neuroscience published by IOS Press, Netherlands. He is a senior member of IEEE.